DOE/ET-53088-367 IFSR #367

Transition from Neoclassical to Turbulent Electron Diffusion

D.E. Kim, Duk-In Choi,* W. Horton, P.N. Yushmanov***
and *V.V. Parail***
Institute for Fusion Studies
The University of Texas at Austin
Austin, Texas 78712

April 1989

* Korea Advanced Institute of Science and Technology, Seoul, Korea
** Kurchatov Institute of Atomic Energy, Moscow, U.S.S.R.

INSTITUTE FOR FUSION STUDIES
THE UNIVERSITY OF TEXAS AT AUSTIN

Robert Lee Moore Hall · Austin, Texas 78712-1060 · (512) 471-1322

June 16, 1989

Professor Fred L. Ribe, Editor,
The Physics of Fluids
University of Washington
356 Benson Hall - BF20
Seattle, Washington 98195

Dear Professor Ribe:

Please find enclosed the typescript "Transition from Neoclassical to Turbulent Electron Diffusion" by D.E. Kim, D.-I. Choi, W. Horton, P.N. Yushmanov, and V.V. Parail. We are submitting this for publication in *The Physics of Fluids.*

Thank you for your consideration of of this work.

Sincerely yours,

Wendell Horton

Wendell Horton

encl: 3 copies typescript

suz

3 copies
send FED-X
WCH has letter
6/14/89

Transition from Neoclassical to Turbulent Electron Diffusion

D.E. Kim and Duk-In Choi
Korea Advanced Institute of Science and Technology
Seoul, Korea
and
W. Horton
Institute for Fusion Studies
The University of Texas at Austin
Austin, Texas 78712
and
P.N. Yushmanov and V.V. Parail
Kurchatov Institute of Atomic Energy
Moscow 123-182, U.S.S.R.

Abstract

Electron diffusion in tokamak geometry is calculated including both the Coulomb collisional pitch angle scattering and the electromagnetic drift wave fluctuation spectrum. In the weak fluctuation limit the neoclassical banana-plateau diffusion coefficient is recovered. At higher fluctuation levels typical of the mixing length amplitude the anomalous transport formulas of drift wave turbulence are recovered.

I. Introduction

The drift motions of electrons in the low frequency electromagnetic drift wave fluctuations[1,2] that are ubiquitous in tokamaks are probably the reason for the measured enhancement of the electron thermal conductivity and particle diffusion rates over the neoclassical rates. The nature of the anomalous transport in the drift waves is a collisionless stochastic diffusion which occurs in the nonlinear particle guiding-center equations of motion.[3,4] The stochastic drift motion has been studied earlier in both the tokamak and simple, local geometries[5,6,7] in the collisionless approximation. The question naturally arises, however, as to the role of the finite time between collisions which limits the Hamiltonian description for the guiding-center motion.

Earlier studies of the Hamiltonian guiding-center motion for the electrons show the onset of diffusion in the presence of two drift waves. The two drift wave study of orbital stochasticity for the sheared slab by Robertson et al.[6] models the description of the passing electrons. The two drift wave study of guiding-center motion for $k_{||} = 0$ modes[5,7] models the description of trapped electrons. In these studies the details of the KAM surfaces and the overlapping resonance condition, that generalize the classical Chirikov overlap condition[8] for motion in longitudinal waves, are developed. Subsequently, Parail and Yushmanov[4] have shown that in the case of a single electromagnetic drift wave where the scalar potential Φ and parallel vector potential $A_{||}$ have different drift surfaces $\hat{\mathbf{b}} \cdot \nabla\Phi \times \nabla A_{||} \neq 0$, the trapped particle motion of an electron in a single wave becomes stochastic due to the competition from the $\mathbf{E} \times \mathbf{B}$ drift and the $v_{||}(t)\delta\mathbf{B}$ drift motion.

All of these physical processes were incorporated in a recent joint study by Horton and Choi with Yushmanov and Parail in a collisionless, toroidal calculation.[3] In that work a low order, isotropic $\mathbf{k}$ space with a power law spectrum spanning the space scales from

$\rho_s = c_s/\omega_{ci}$ to $1/k_{\max} \ll \delta_s = c/\omega_{pe}$ was used to represent the electromagnetic drift wave fluctuations. The Horton et al.[3] study showed that in general the trapped electron diffusion was considerably stronger than the passing electron diffusion. The results of the collisionless stochastic diffusion in the model fluctuation spectrum where found to be given by

$$D = c_1 \varepsilon^{1/2} \frac{c^2 \omega_{be}}{\omega_{pe}^2} + c_2 \varepsilon^{1/2} \frac{\rho_s}{r_n} \frac{cT_e}{eB} \tag{1}$$

where $\varepsilon^{1/2}$ is the fraction of trapped electrons, the c_1 contribution arises from the smaller scale c/ω_{pe} part of the fluctuation spectrum, and the c_2 contribution from the larger scale c_s/ω_{ci} part of the fluctuation spectrum. The relative strength c_2/c_1 depends principally on the shape of the fluctuation spectrum, as well as other detailed considerations. For a typical spectral index and mixing length amplitude level it was found that $c_1 \leq 1$ and $c_2 \leq 2-3$. In the actual tokamak experiment, however, the Coulomb 90° scattering rate ν_e with ions and impurities changes trapped electrons into passing electrons at the rate $\nu_{\text{eff}} = \nu_e/\varepsilon$. Even at the highest temperatures and lowest densities the number of bounce periods for a single electron is probably limited to $\omega_{be}/\nu_{\text{eff}} \leq 10^3$. Thus, it becomes important to understand the effect of the finite pitch angle scattering rate ν_e on the anomalous diffusion of the electrons.

In the present work we re-investigate this problem by expanding the model in Ref. 3 to allow for the finite time between collisions. Introducing the Coulomb collisional scattering of the electrons through elastic pitch angle scattering in guiding-center motion allows the model to take into account the finite lifetime of the trapped electron. It also allows the model to recover the neo-classical diffusion[9] of the electrons in the limit of low fluctuation amplitudes.

The previous Hamiltonian studies suffer from the limitation that to establish a well-defined stochastic diffusion coefficient, it was typically required to follow the electron orbits for the order of $10^2 - 10^3$ bounce periods, greater than the lifetime $1/\nu_{\text{eff}}$ of a trapped orbit.

In this work we follow the electrons in their parallel motion along the magnetic field

assuming the exact conservation of the magnetic moment. The electrons are given frequent, small pitch angle scatterings in velocity space which then allow those particles near the trapped-passing separatrix to scatter out of the trapping region of velocity space at the rate $\nu_{\rm eff} = \nu_e/\varepsilon$ with $\varepsilon = r/R$ measuring the depth of the magnetic well. At sufficiently low fluctuation amplitudes we recover the neoclassical diffusion D_{nc} determined by $\varepsilon^{1/2}\nu_{\rm eff}(v_D/\omega_{be})^2$ for the trapped particle fraction. Here v_D is the electron ∇B-curvature drift velocity and v_D/ω_{be} the radial banana excursion distance of the trapped particle.

For small ε, where the collisionless, parallel motion can be given by the elliptic function, the observed diffusion reproduces the Hinton-Hazeltine banana-plateau formula.[9]

The calculations for the positive, definite microscopic diffusion coefficient

$$D(E) = \lim_{t\to\infty} \frac{1}{N} \sum_{i=1}^{N} \frac{(x_i(t) - x_i(0))^2}{2t} \tag{2}$$

determine the diffusion rate of each energy E component of the electron spectrum.

The work is organized as follows: In Sec. II the guiding-center equations of motion, the collisionless Hamiltonian and the pitch angle scattering operator are described. In Sec. III the results of the integration of the guiding-center motion and the parametric dependence of the anomalous and neoclassical diffusion rates are presented. In Sec. IV the results are summarized in conclusion.

II. Electron Guiding-Center Dynamics

The motion of an electron in fluctuations with frequency components $\omega \ll \omega_{ce} = eB/m_e c$ and wavelengths $k_\perp \rho_e \ll 1$ where $\rho_e = v_e/\omega_{ce}$ is described by the guiding-center equations of motion

$$\frac{d\mathbf{x}}{dt} = v_\parallel \frac{\mathbf{B}}{B} + \frac{c\mathbf{b}\times\nabla\Phi}{B} + \frac{cm}{qB^2}\left(\frac{1}{2}v_\perp^2 + v_\parallel^2\right)\mathbf{b}\times\nabla B \tag{3}$$

$$\frac{dv_\parallel}{dt} = -\mu\mathbf{b}\cdot\nabla B + \frac{q}{m}E_\parallel \tag{4}$$

where $\mu = v_\perp^2/2B$ is a constant of the motion. In the presence of electromagnetic drift wave fluctuations

$$\mathbf{E}(\mathbf{x},t) = -\nabla\Phi - \frac{\hat{\mathbf{b}}}{c}\frac{\partial A}{\partial t} \tag{5}$$

$$\delta\mathbf{B} = \nabla A \times \hat{\mathbf{b}} \tag{6}$$

where Φ is the scalar potential and A the parallel component of the vector potential, the unit vector $\hat{\mathbf{b}}$ following the magnetic field line has the ambient or mean component $\hat{\mathbf{b}}_0$ and the fluctuating component $\delta\mathbf{B}/B_0$. In the limit of small $\delta B_\perp/B_0 \ll 1$ the unit vector reduces to

$$\hat{\mathbf{b}} = \hat{\mathbf{b}}_0 + \frac{\delta\mathbf{B}_\perp}{B_0}\,. \tag{7}$$

Neglecting the finite shift of toroidal magnetic surfaces the mean field is

$$\mathbf{B} = \left(B_p h\hat{\boldsymbol{\phi}} + B_\theta(r)\hat{\boldsymbol{\theta}}\right)/(1+\varepsilon\cos\theta) \tag{8}$$

where $\varepsilon = r/R$.

We measure the helical pitch due to the toroidal current with

$$q(r) = \frac{rB_\phi}{RB_\theta}\,, \tag{9}$$

and compute from the ambient field that

$$\hat{\mathbf{b}}_0 = \hat{\boldsymbol{\phi}} + \frac{\varepsilon}{q}\hat{\boldsymbol{\theta}} \qquad B = B_0\hat{B}(r,\theta)$$

$$\hat{B}(r,\theta) = (1+\varepsilon\cos\theta)^{-1}\,. \tag{10}$$

With $\epsilon = \frac{1}{2}v^2$ and $\lambda = \mu B_0/\epsilon$ we also have

$$\mathbf{v}_D = -\frac{mc\epsilon(2-\lambda\hat{B})}{eB_0R}\left(\hat{\boldsymbol{\theta}}\cos\theta + \hat{\mathbf{r}}\sin\theta\right) \tag{11}$$

$$v_\parallel = \sigma(2\epsilon)^{1/2}(1-\lambda\hat{B})^{1/2} \tag{12}$$

where $\sigma = \pm 1$.

For drift modes with $k_{||} \sim 1/qR$ and $\omega \sim k_{\perp}(cT/eBa)$ the parallel acceleration from the mirror force greatly exceeds that of $qE_{||}/m$ from the fluctuation. In the approximation where $E_{||}$ is neglected the system becomes

$$\dot{\theta} = \frac{v_{||}}{qR} = \sigma \frac{(2\epsilon)^{1/2}}{qR}(1 - \lambda \widehat{B})^{1/2} \tag{13}$$

$$\dot{v}_{||} = -\frac{\lambda \epsilon \widehat{B}^2 \sin\theta}{qR} \tag{14}$$

and in the local cross-field coordinates $x = r(t) - r_0$, $y = r_0\theta$

$$\dot{x} = -\frac{\partial H}{\partial y}\left(x, y, \theta(t), v_{||}(t), t\right) \tag{15}$$

$$\dot{y} = \frac{\partial H}{\partial x}\left(x, y, \theta(t), v_{||}(t), t\right) . \tag{16}$$

The system (13)–(16) is the $1\frac{1}{2}$-D Hamiltonian dynamics introduced in Ref. 3 for calculating the stochastic electron diffusion. The effective Hamiltonian is

$$H = \widetilde{H} + H_D = \frac{c}{B}\left[\varphi(x, y, t) - \frac{v_{||}(t)}{c} A(x, y, t)\right] + v_D r \cos\left(\theta(t) + y/r_0\right) . \tag{17}$$

The effect of magnetic shear is included in A by writing

$$A = \frac{1}{2} A_s x^2 + A(x, y, t)$$

where $A_s = B_s/x = (B_0/qR)(d\ln\, q/d\ln\, r)$.

For the fluctuation spectrum we adopt the same model used in Ref. 3 and do not repeat here the detailed argument given for the spectrum. The electrostatic potential is represented by an isotropic truncated power with $\mathrm{k}_{\perp} = (nk_1, mk_1)$, $(n, m = 1, \ldots, N)$ and $c\Phi_{\mathrm{k}}/B = (\delta_s^2 \omega_{be})\phi_1/|\mathrm{k}_{\perp}|^{m_\phi}$. The resulting model for the dimensionless fluctuations is

$$\phi(x, y, t) = \phi_1 \sum_{\mathbf{k}} \frac{1}{k^{m_\phi}} \sin(k_x x + \alpha_k) \cos\left(k_y(y - ut) + \beta_k\right)$$

and the Hamiltonian is

$$\tilde{h}(x,y,t) \;=\; \phi(x,y,t) + \gamma\dot{\theta}(t)A(x,y,t) \tag{18}$$

where u is the phase velocity m_ϕ and m_A is spectral indices, and $\{\alpha_{\mathbf{k}}, \beta_{\mathbf{k}}\}$ are random phases. The parameter ϕ_1 is the dimensionless amplitude and the parameter γ measures the particle coupling to the parallel vector potential with

$$\gamma\dot{\theta} = \frac{\overline{k}_{\|} v_{\|}}{\omega_{\mathbf{k}}} = \frac{B_s v_{\|}(t)}{B_0 u} \; . \tag{19}$$

The details of the calculations and values of $u, \gamma, \phi_1, m_\phi$ are given in Ref. 3.

In the present study we use the collisionless Ohm's law[3] to relate $\phi_{\mathbf{k}}$ and $A_{\mathbf{k}}$ and as the result we have

$$\tilde{h}(x,y,t) = \phi_1 \sum_{\mathbf{k}} \frac{1}{k^{m_\phi}} \left[1 + \frac{\gamma\dot{\theta}(t)}{1+k^2}\right] \sin(k_x x + \alpha_k) \cos\left(k_y(y-ut) + \beta_k\right) \; .$$

In Eq. (18) and the following we use the dimensionless space time variables given by

$$\frac{\omega_{pe}}{c} x \rightarrow x \qquad \frac{\omega_{pe}}{c} y \rightarrow y \qquad \omega_{be} t \rightarrow t$$

where $\omega_{be} = v_e \varepsilon^{1/2}/qR$. The root-mean-square level $\tilde{\varphi}$ of the fluctuation spectrum is given by

$$\tilde{\varphi} = \frac{1}{2}\phi_1 \left[\sum_{\mathbf{k}} \left(k^{-2m_\phi}\right)\right]^{1/2} \; . \tag{20}$$

The $\mathbf{E} \times \mathbf{B}$ nonlinear circulation frequency $\Omega_{\mathbf{k}}$ is given by

$$\Omega_{\mathbf{k}} = \frac{c k_\perp^2 \Phi_{\mathbf{k}}}{B} = \frac{\omega_{be} k^2 \phi_1}{k^{m_\phi}} \; . \tag{21}$$

The ratio of the nonlinear circulation frequency $\Omega_{\mathbf{k}}$ at the scale wavenumber k is

$$\frac{\Omega_{\mathbf{k}}}{\omega_{be}} = \frac{\phi_1}{k^{m_\phi - 2}} \; . \tag{22}$$

We take $m_\phi = 2$ as the reference spectrum in which $\Omega_{\mathbf{k}}$ is constant and equal to $\omega_{be}\phi_1$. The parameter $\Omega_{\mathbf{k}}/\omega_{be}$ determines the stochasticity due to the ω_{be} and $\mathbf{E} \times \mathbf{B}$ overlapping resonances. For $\Omega_{\mathbf{k}} \ll \omega_{be}$ the motion is integrable in the model Hamiltonian (18).

In the dimensionless variables the Hamiltonian motion in Eqs. (15) and (16) reduces to

$$\begin{aligned} \frac{dx}{dt} &= -\frac{\partial \tilde{h}}{\partial y} + v_D \sin\theta \\ \frac{dy}{dt} &= \frac{\partial \tilde{h}}{\partial x} + v_D \cos\theta + u + v_s x \end{aligned} \tag{23}$$

which is written in the wave frame $y \to y - ut$.

Here we relate the electromagnetic amplitude parameter ϕ_1 to the electrostatic drift wave parameter $\phi_{\rm ML}$. We define $\phi_{\rm ML}$ as the dimensionless mixing length parameter[1,2] in the formula

$$\frac{e\Phi_{\mathbf{k}}}{T_e} = \frac{\phi_{\rm ML}}{k_x r_n} = \frac{\delta_s}{r_n}\frac{\phi_{\rm ML}}{k} \tag{24}$$

with $k = k_x c/\omega_{pe}$, $r_n = |d\ln N/dr|^{-1}$ and $\delta_s = c/\omega_{pe}$. For relating ϕ_1 to $\phi_{\rm ML}$ it is convenient to introduce the MHD ballooning mode pressure limit stability parameter α_p

$$\alpha_p = \frac{2q^2\beta_e}{\varepsilon_n} \tag{25}$$

where the ballooning stability limit (for $\eta_i = \eta_e = 0$) is $\alpha_p \leq 0.8 s^{1/2}$ with $s = d\ln q/d\ln r$, $\varepsilon_n = r_n/R$. Using $\rho_s/\delta_s = (m_i\beta_e/2m_e)^{1/2}$ we find that

$$\frac{\Omega_{\mathbf{k}}}{\omega_{be}} = \phi_1 = \frac{\alpha_p^{1/2}}{2(\varepsilon\varepsilon_n)^{1/2}}\phi_{\rm ML} \tag{26}$$

so that $\phi_{\rm ML} \sim 1$ implies $\phi_1 \geq 1$ provided $\alpha_p > 4\varepsilon\varepsilon_n$ which is typical.

For $\alpha_p \leq 1$ then $\phi_1 > 1$ for $\phi_{\rm ML} > 2(\varepsilon\varepsilon_n)^{1/2}$. We consider the range $0 \leq \phi_1 \leq 5$ as relevant to the tokamak experiments. The dimensionless drift velocity in Eq. (23) is

$$\frac{v_D}{\delta_s\omega_{be}} = \left(\frac{q^2 2\beta_e}{\varepsilon}\right)^{1/2} \sim \alpha_p^{1/2}\,. \tag{27}$$

The asymptotic banana diffusion rate is

$$D_{nc}^b = \varepsilon^{1/2}\nu_{\rm eff} q^2 \rho_e^2/\varepsilon\,,$$

and in units of $\delta_s^2\omega_{be}$ it is

$$D_{nc}^b/\delta_s^2\omega_{be} = \nu_{*e}\left(\frac{q^2\beta_e}{2\sqrt{\varepsilon}_n}\right) = \frac{\varepsilon_n}{4\sqrt{\varepsilon}}\,\nu_{*e}\alpha_p\ , \tag{28}$$

where $\nu_{*e} = \nu_{\rm eff}/\omega_{be} = \nu_e\, qR/\varepsilon^{3/2}\, v_e$.

Coulomb interactions of the electrons with the ions and impurities gives the effective 90° angular scattering rate

$$\nu_e = \frac{4\pi n_e Z e^4}{m_e^2 v^3}\ln\Lambda \tag{29}$$

where $Z = \sum_i n_i Z_i^2/n_e$ and $\ln\Lambda$ is the Coulomb logarithm taking into account multiple small scatterings. The scattering rate (29) is taken into account through a rotation of the velocity vector $\mathbf{v} \rightarrow \mathbf{v}'$ with $\cos\gamma = \mathbf{v}\cdot\mathbf{v}'/v^2$. At each time step Δt the small, random angle γ is taken from

$$\gamma = [-\nu_e\Delta t\,\ln(1-\eta)]^{1/2}$$

where η is randomly distributed on [0,1] and $\nu_e\Delta t \ll 1$ is applied to the pitch angle variable $\xi = v_{||}/v$ in such a way as to produce the diffusion

$$\frac{\partial f}{\partial t} = \frac{\nu_e}{2}\frac{\partial}{\partial\xi}(1-\xi^2)\frac{\partial f}{\partial\xi}\ . \tag{30}$$

In terms of the θ,ξ variables the parallel particle motion from Eqs. (13) and (14) is

$$\dot\theta = \omega_T\xi \qquad \dot\xi \ = \ -\frac{\omega_T(1-\xi^2)}{2\hat B}\frac{\partial\hat B}{\partial\theta} \tag{31}$$

where

$$\omega_T \ = \ \frac{v_e}{qR}\ . \tag{32}$$

While θ,ξ are convenient variables for the numerical integration of the parallel motion, the theoretical analysis is often more convenient with the magnetic moment per unit of energy λ, that is, the invariant of the parallel motion in Eq. (31), $\lambda_\xi\dot\xi + \lambda_\theta\dot\theta = 0$,

$$\lambda = \frac{1-\xi^2}{\hat B(\theta)} \qquad \text{and} \qquad \xi = \sigma(1-\lambda\hat B)^{1/2} \tag{33}$$

where $\sigma = \pm 1$ gives the branch of $v_{||}$. The distribution f_σ of N particles in the variables x, y, θ, λ satisfies

$$\frac{\partial f_\sigma}{\partial t}(x,y,\theta,\lambda,t) \;+\; \frac{\partial h}{\partial x}\frac{\partial f_\sigma}{\partial y} - \frac{\partial h}{\partial y}\frac{\partial f_\sigma}{\partial x} + \sigma\omega_T\xi\frac{\partial f_\sigma}{\partial\theta}$$

$$= 2\nu\,\frac{(1-\lambda\hat{B})^{1/2}}{\hat{B}}\,\frac{\partial}{\partial\lambda}\left[\lambda(1-\lambda\hat{B})^{1/2}\right]\frac{\partial f_\sigma}{\partial\lambda} \tag{34}$$

where the energy per unit mass $\epsilon = E/m = \frac{1}{2}v^2$ is a parameter in the motion.

When the equilibrium drift motion dominates the $\mathbf{E}\times\mathbf{B}$ and $v_{||}\delta\mathbf{B}$ drift motion $\nabla h_D \gg \nabla\tilde{h}$ the distribution functions from Eq. (34) reduce to the neoclassical distribution which is approximately

$$f \cong f_0(\epsilon,x) + \frac{v_D\sigma(2)^{3/2}(\cos\theta-\cos\theta_T)^{1/2}}{\omega_b}\frac{\partial f}{\partial x} + \frac{2\nu v_D\theta}{\omega_{be}^2}\frac{\partial f}{\partial x} \tag{35}$$

for trapped particles. The net radial flux of particles with given ϵ is obtained from $\int d\theta \int d\lambda\hat{B}(1-\lambda\hat{B})^{1/2}v_D\sin\theta f$ and given by

$$D_{nc} = \varepsilon^{1/2}\frac{\nu_{\rm eff}v_D^2}{\omega_{be}^2}K_{11}(\nu_{*e},\varepsilon) = \varepsilon^{1/2}\left(\frac{q^2\beta_e}{2\varepsilon}\right)\nu_{*e}K_{11}(\nu_{*e},\varepsilon)\left[\frac{\omega_{be}c^2}{\omega_{pe}^2}\right], \tag{36}$$

where K_{11} is a dimensionless function of order one in the banana regime $\nu_{*e} \ll 1$.

For the Lorentz collision operator, the function K_{11} is given by Hinton-Hazeltine[9] as

$$K_{11} = K_{11}^{(0)}\left[1 + a\nu_{*e}^{1/2} + b\nu_{*e}\right]^{-1} \tag{37}$$

with $K_{11}^{(0)} = 1.04$, $a = 2.01$ and $b = 1.53$ for $\varepsilon \ll 1$. The $a\nu_{*e}^{1/2}$ correction is obtained from the boundary layer particles with $\dot{\theta} \simeq v\Delta\xi/qR \simeq \nu/(\Delta\xi^2)$ such that $\Delta v_{||}/v = \Delta\xi = (\nu/\omega_T)^{1/3}$ which is order of the magnetic well depth $\Delta v_{11}/v \sim \varepsilon^{1/2}$ when $\nu_{*e} \sim 1.0$. The formula (37) (and the large ε version in Eq. (6.125) of Ref. 9) is obtained by a least square fitting in the range $10^{-2} \le \nu_{*e} \le 10$ of the numerical analysis of the transitional regime in Hinton and Rosenbluth.[10] The analysis is restricted to small ε.

In Fig. 1 we show the results of our statistical simulation of the neoclassical problem for a distribution of 64 particles with $\varepsilon = 1/4$. The solid line gives the results from (36)–(37) and the vertical lines the simulation values along with the standard deviation from the fluctuations in D. The simulation is in good agreement with Eqs. (36)–(37) for ν_{*e} in the range 10^{-2} to 10. In addition we have tested the v_D dependence of the measured neoclassical diffusion and find good agreement with

$$D_{nc} = 0.110 v_D^{2\pm\delta} \qquad \text{with} \qquad \delta \lesssim 0.005$$

at $\nu_* = 0.0865$ and $\varepsilon = 0.25$.

III. Anomalous Transport Properties

In this section we describe the parametric dependence of microscopic diffusion coefficient $D_m(p_n)$ where

$$\{p_n\} = \{\tilde{\varphi}, m, u, v_D, \nu_*, \varepsilon, v_s, \beta_e\} \ ,$$

and we discuss the statistical properties of the measured transport.

We find that the x-motion is well described as a diffusion process. For typical parameters we show in Fig. 2 the time dependence of the variance of the x-motion for a string of 32 particles starting at $x = x_0$ and $k_1 y_i = 2\pi(i-1)/N$ with $i = 1, 2, \ldots N$. The variance

$$\sigma_x(t) = \frac{1}{N} \sum_{i=1}^{N} (x_i(t) - x(0))^2 \tag{38}$$

in Fig. 2(a) shows a clean linear increase in time after a small number of bounce periods except at the largest ($\tilde{\varphi} = 7, 9$) values of the turbulent field where some oscillations in $\sigma_x(t)$ appear.

The running diffusion coefficient

$$D_m(t) = \frac{\sigma_x(t)}{2t} = \frac{1}{2t} \frac{1}{N} \sum_{i=1}^{N} (x(t) - x_i(0))^2 \tag{39}$$

given in Fig. 2(b) shows a well-defined D_m except at the largest values of $\tilde{\varphi} = 7, 9$ where the oscillations of $D_m(t)$ about $\overline{D}_m$ produce the significant root-mean-square deviations $\delta D = \left[\overline{(D_m(t) - \overline{D}_m)^2}\right]^{1/2}$ found in some of the following graphs showing $\overline{D}_m \pm \delta D_m$ against a parameter. Here we use $\langle\ \rangle$ for the average over the distribution of particles and $\overline{A}$ for the time average.

The variation of $\overline{D}_N$ with N is studied and found to decrease as $1/N^{1/2}$. Thus, we are able to obtain reasonable accuracies of order 20%, 12%, and 8% with 32, 64, and 128 particles. In Fig. 3 we show the dependence of $\overline{D}_m$ with $\tilde{\varphi}$ and ε. On the scale of $\tilde{\varphi}$ shown the increase of $\overline{D}_m(\tilde{\varphi})$ is linear almost immediately and continues until $\tilde{\varphi} \sim 10 - 12$ and then begins to oscillate with between 1 and 2 as found earlier in Ref. 3, 5, and 7. In high amplitude regime the $\mathbf{E} \times \mathbf{B}$ circulation frequency $\Omega_{\mathbf{k}}$ is considerably greater than the electron bounce frequency and it becomes time consuming to calculate $\overline{D}_m$ as noted in earlier works on $\mathbf{E} \times \mathbf{B}$ stochastic transport. The amplitude beyond $\tilde{\varphi} = 5$, however, are probably well above those expected in the tokamaks. Below this regime $\Omega_{\mathbf{k}} \leq \omega_{be}$ the linear increase of $\overline{D}_m = D_1\tilde{\varphi}$ with $\tilde{\varphi}$ is consistent with renormalized propagator theory of stochastic transport. Also we note that the maximum of $\overline{D}_m$ in Fig. 3 is about 2 while the maximum of $\overline{D}_m$ measured in Ref. 3, which considers only trapped particles, is about 3. In the present case we included all passing and trapped particles, while in Ref. 3 the contribution from the passing particles to the transport is neglected. They considered only trapped particles and calculated the transport by multiplying the trapped particle fraction ($\sim \varepsilon^{1/2}$) to the observed $\overline{D}_m$. Therefore, our results and theirs should differ in magnitude of transport by factor of $\sqrt{\varepsilon} \simeq 0.5$ which is similar to the 2/3 ratio from the present calculations. The slight enhancement over 0.5 can be ascribed to the fact that passing particles that are close to the separatrix also contribute to the transport.

At fixed $\tilde{\varphi}$ the diffusion coefficient increases[12] with increasing collisionality ν_{*e}. The increment of $\overline{D}_m$ with ν_{*e} is shown in Fig. 4. The straight line is the least square fit to the

data as

$$\overline{D}_m(\nu_{*e}) = 1.26(1 + 0.325\nu_{*e}) \ . \tag{40}$$

In the high collisionality regime, the electrons are significantly scattered in pitch angle in each bounce period. The collisions change the pitch angle and thus the $\tilde{h}(x, y, v_{\|}, t)$ drift surface of the electrons producing an anomalous diffusion proportional to the collision frequency. Although some theory for $\overline{D}_m$ can be developed, we do not attempt it here. Detailed analysis as well as a theory to understand $\overline{D}_m$ is presently under active study and will be reported elsewhere.

In Fig. 5 we show the effect of shear on the anomalous transport. It shows rapid reduction with increasing electron velocity due to shear. The role of shear velocity on the anomalous transport is to impose the directionality of the particle flow in the phase space. Thus, the system becomes less stochastic when shear velocities are present. In our case, shear velocities are included in the form of $v_s x$ and the presence of finite v_s induces a strong directional flow in the phase space for large x. This strong directional flow for large x takes the role of a barrier for particles diffusing radially. Thus, they affect the transport significantly and reduce $\overline{D}_m$ very rapidly with increasing v_s. This feature of the reduction of transport with increasing shear is recently utilized successfully to fit a large confinement database by Kesner.[13]

To see the effect of collisions, we plotted the location of particles in (λ, θ) space. Initially, particles are positioned in constant $\lambda(\equiv \mu B_0/\epsilon)$ and equidistantly along θ. When we integrated the equations of motion without collisions, this string of particles remain on this constant initial λ string because λ is constant of motion of our equation of motion. When collisions are introduced, the particles scatter and fill the entire accessible phase space within a few $1/\nu_{\text{eff}}$ time. Figure 6(b) is a snapshot of the system of particles in (λ, θ) space when about $3/\nu_{\text{eff}}$ is elapsed. We note that the particles are nearly uniformly spread over the full accessible space. As shown in Fig. 6(c), which is a snapshot of the system when about $8/\nu_{\text{eff}}$ is elapsed, the particles completely fill the space showing the effect of collisions.

IV. Conclusions

In the low collisionality or banana regime the electron transport is dominated by the stochastic plateau from trapped electrons.

In the collisionless plateau there are two competing mechanisms as reported earlier[3] giving $\chi_{em}^{(1)} + \chi_{es}^{(2)}$. Using the shear dependence of the diffusion as shown in Fig. 5 Kesner[13] gives a model thermal diffusivity for the interior plasma that predicts well the energy confinement time in a large tokamak database. The diffusivity formula is not large enough to explain the edge plasma transport which is semi-collisional.

In the semi-collisional or collisional plateau regime there is an additional anomalous flux contribution proportional to the collision frequency given by

$$\chi^{(3)} \simeq C\nu_{ei}\frac{c^2}{\omega_{pe}^2},$$

which may explain the large edge transport observed in tokamaks as analyzed by Yushmanov and Parail.[12].

Well into the banana regime the principal loss mechanism is the stochastic diffusion of the trapped particles. In the banana-plateau transitional region the losses arise from a much larger region of pitch angles, since collisions can prevent a transiting electron from completing its revolution around the magnetic axis. Only those electrons that can complete several rotations around the magnetic axis can average out the effect of the radial ∇B-curvature drift and the fluctuating drift velocity $\hat{\mathrm{b}} \times \nabla\tilde{h}$.

In terms of the transitional particles and the boundary layer effects associated with collisional crossing and stochastic layers along the separatrix between trapped and circulating electrons more detailed theoretical and simulations studied may be required. The formulation of the guiding-center Hamiltonian then becomes $H(x, y, \theta, v_{||}, t)$ with $2\frac{1}{2}$ degrees of freedom. Theoretically this can allow the process of Arnold diffusion along the resonant webbs in the 4d phase space, in principle, to increase the diffusion rate. In our view, the role of collisions

is sufficiently strong as to prevent the formation or practical importance of these long-time limit Hamiltonian structures. In contrast, the stochasticity of the $1\frac{1}{2}$ D Hamiltonian is clearly important for actual tokamak experiments once the fluctuation level becomes such that $\tilde{v}_\perp = |\nabla\tilde{h}| > v_D$ the ∇B-curvature drift velocity. The stochasticity arises both from the $\Delta\omega$ of the fluctuation spectrum which resonates with the $\mathbf{E}\times\mathbf{B}$ circulation frequency and from the ω_{be} frequency of the parallel motion resonating with smaller scale $\mathbf{E}\times\mathbf{B}$ and $k_{||}^{nl}v_{||}$ circulation frequencies. This work shows that the actual motion of electrons in tokamak traps to be complex trajectories with structure on at least three space-time scales.

Acknowledgments

This work was supported by NSF Grant #Int-8617403 and the U.S. Department of Energy contract #DE-FG05-80ET-53088. This work was also supported partially by NSF-KOSEF International Collaborative Research.

References

1. W. Horton and R.D. Estes, Nucl. Fusion **19**, 203 (1979).

2. P.C. Liewer, Nucl. Fusion **25**, 543 (1985).

3. W. Horton, D-I. Choi, P:.N. Yushmanov and V.V. Parail, Plasma Physics **29**, 901 (1987).

4. V.V. Parail and P.N. Yushmanov, JETP Letts. **42**, 343 (1985).

5. W. Horton, Plasma Phys. **27**, 937 (1985).

6. J.A. Robertson, W. Horton, and D-I. Choi, Phys. Fluids **30**, 1059 (1987).

7. R.G. Kleva and J.F. Drake, Phys. Fluids **27**, 1686 (1984).

8. B.V. Chirikov, Phys. Rep. **52**, 263 (1979).

9. F.L. Hinton and R.D. Hazeltine, Rev. Mod. Phys. **48**, 239-308 (1976).

10. F.L. Hinton and M.N. Rosenbluth, Phys. Fluids **16**, 836 (1973).

11. W. Horton and D.-I. Choi, Phys. Rep. **49**, 273 (1979).

12. V.V. Parail and P.N. Yushmanov, "The Dynamics of the Additional Heating and the Profile Effects in a Tokamak," D-I-1, Twelfth IAEA Conference on Plasma Physics and Controlled Fusion Research, Nice, France (1988).

13. J. Kesner, "Scaling of Ohmic and Auxiliary Heated Tokamaks," PFC/JA-88-38, MIT Report and Sherwood Theory Conference, San Antonio, TX, April 3-5, 1989, 2B5.

Figure Captions

1. Comparison of neoclassical diffusion coefficient D_{nc} with the numerical simulation for $\varepsilon = 0.25$ and $\beta_e = .01$. Solid curve is the Hinton-Hazeltine banana-plateau transitional formula and the vertical lines are the mean and rms-deviation from the simulation.

2. Time dependence of the x-variance and the running diffusion coefficient for $\tilde{\varphi} = 0, 1, 3, 5, 7, 9$. (a) Variance $\sigma_x = (N)^{-1} \sum_i (x_i(t) - x_i(0))^2$; (b) Running diffusion coefficient $D = \sigma_x(t)/(2t)$.

3. Dependence of $\overline{D}$ on the amplitude $\tilde{\varphi}$ (root-mean-square) at fixed collisionality $\nu_{*_e} = 0.186$.

4. Dependence of $\overline{D}$ on collisionality ν_{*_e} at fixed $\tilde{\varphi} = 5.0$.

5. Dependence of $\overline{D}$ on shear v_s at fixed $\tilde{\varphi} = 5.0$.

6. Collisional evolution of a string of trapped electrons placed at $\lambda = 1.0$ in tokamak with $\varepsilon = 0.25$ and $\nu_* = 0.186$. Distribution at (a) initial string, (b) $t = 3/\nu_{\text{eff}}$ and (c) at $t = 8/\nu_{\text{eff}}$ in λ, θ space.

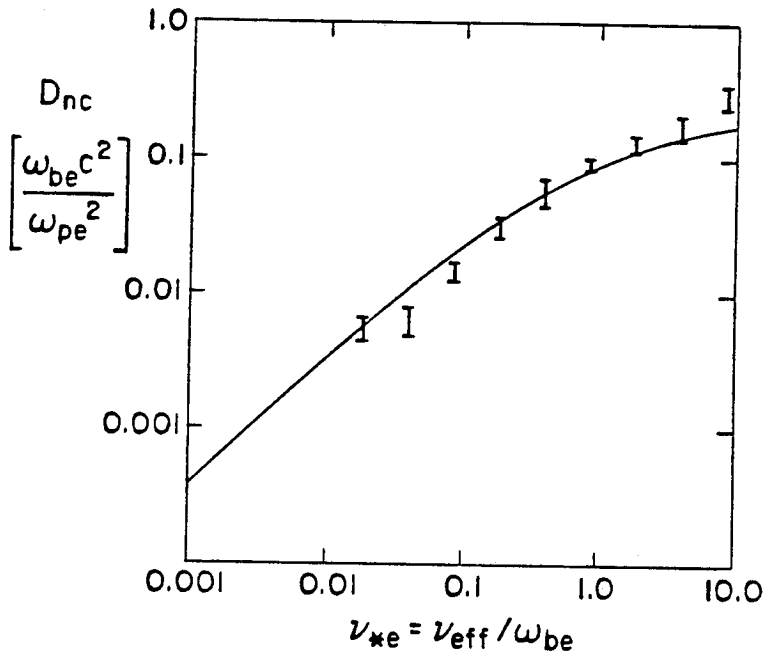
1.0
D_{nc}
$\left[\frac{\omega_{be}c^2}{\omega_{pe}^2}\right]$
0.1
0.01
0.001
0.001
0.01
0.1
1.0
10.0
$\nu_{*e} = \nu_{eff}/\omega_{be}$

Fig. 1

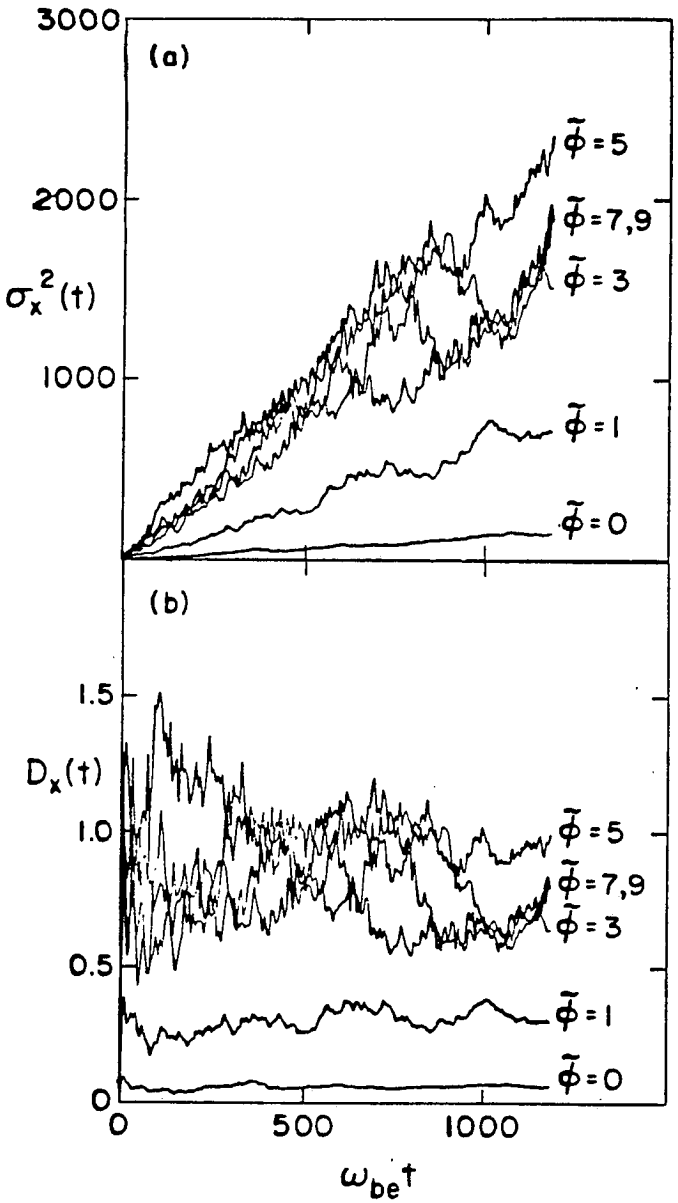
3000
2000
1000
(a)
$\sigma_x^2(t)$
$\tilde{\Phi}=5$
$\tilde{\Phi}=7,9$
$\tilde{\Phi}=3$
$\tilde{\Phi}=1$
$\tilde{\Phi}=0$
(b)
1.5
1.0
0.5
0
$D_x(t)$
$\tilde{\Phi}=5$
$\tilde{\Phi}=7,9$
$\tilde{\Phi}=3$
$\tilde{\Phi}=1$
$\tilde{\Phi}=0$
0
500
1000
$\omega_{be}t$

Fig. 2

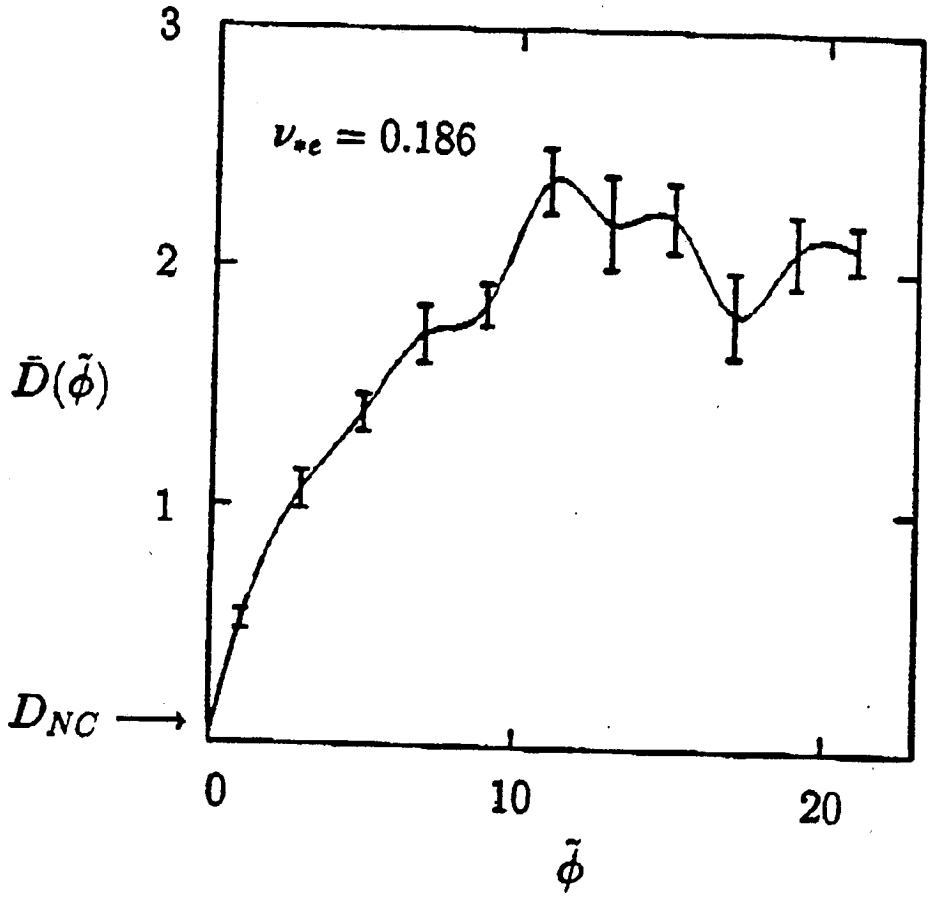

Fig. 3

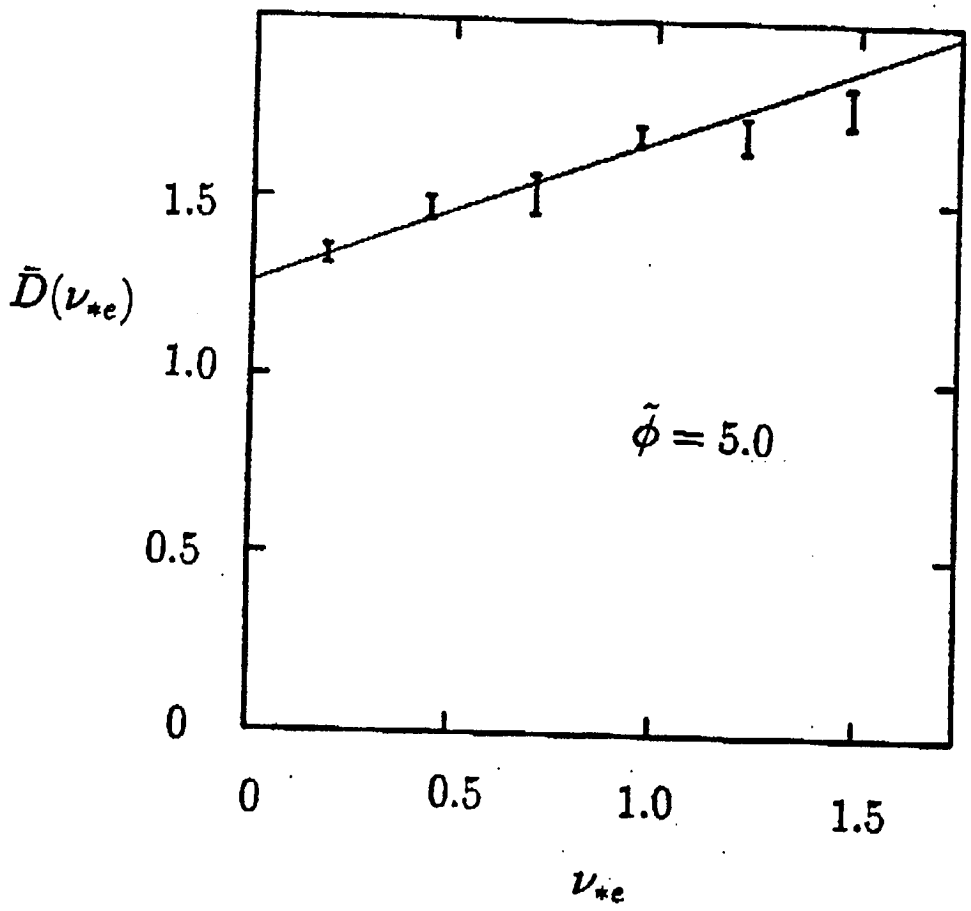

Fig. 4

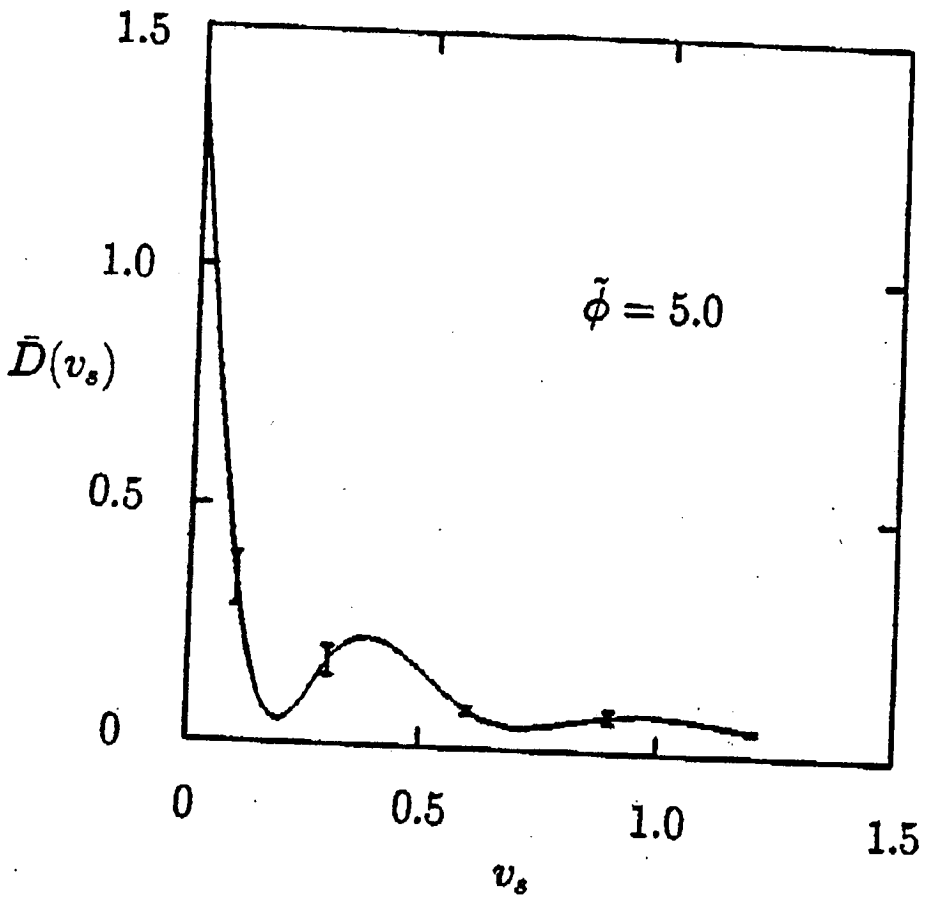

Fig. 5

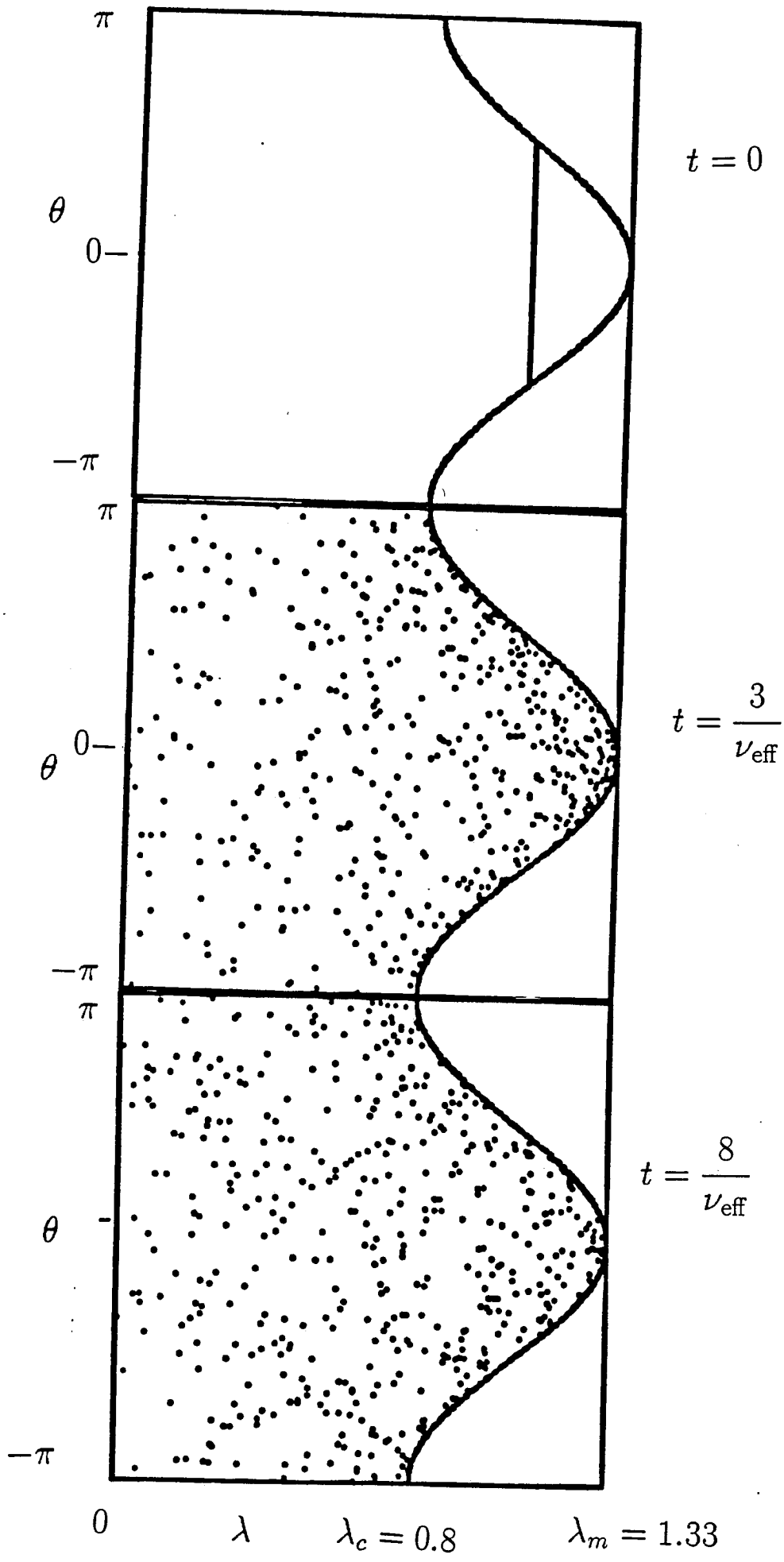

Fig. 6